



# Memory-free loading paths for a coupled continuous contact problem with friction

N. Cwiekala<sup>a,\*</sup>, J.R. Barber<sup>b</sup>, D.A. Hills<sup>a</sup>

<sup>a</sup> Department of Engineering Science, University of Oxford, Parks Road, OX1 3PJ Oxford, United Kingdom

<sup>b</sup> Department of Mechanical Engineering, University of Michigan, Ann Arbor, MI 48109-2125, USA

## ARTICLE INFO

### Keywords:

Coupled contact  
Memory-free  
Partial slip  
Distributed dislocations  
Shakedown

## ABSTRACT

The plane elastic problem of a circular disk shrink fitted into a hole in an elastically similar plane, with a frictional interface, is studied subject to the application of a radial force and torque both of which vary with time. This is done by the use of edge dislocation distributions to represent slip. The evolution of extent and position of a slip zone as well as the magnitude of slip displacements is studied. Conditions for continuous slip, leading a history or load path independent solution are derived. The results derived prepare for the study of the shakedown behaviour of a continuous coupled contact.

## 1. Introduction

Contacts potentially in partial slip arise in many mechanical assemblies, some very complicated such as a gas turbine. Contacts are often subjected to a constant component of load (such as bolt tightening) or slowly varying load (such as the centrifugal forces developed in the engine) together with a high frequency oscillatory component, normally originating in vibration. Where there is slip in the steady state the conditions are ripe for crack nucleation – so called fretting fatigue – but, on the other hand, the cyclic slip absorbs energy and therefore causes damping, limiting the severity of the effect. If the contact starts off in partial slip but later becomes stuck, owing to the development of locked-in interfacial slip displacements with attendant tractions, it is said to ‘shake down’, a term borrowed from plasticity theory where it implies the evolution of an initial elastic–plastic phase to an elastic steady state. Contacts which are fully stuck may actually have a slightly higher stress concentration at their edges but do not suffer from surface degradation, and they also, evidently, do not damp energy. One ambition of the gas turbine industry is to produce a ‘whole engine model’ in which, at some level of fidelity, all joints or contacts are included, and it would be valuable to know if, in the steady state, they are adhered or suffering cyclic slip.

One possible method of analysis is simply to form a model of the contact and track out the evolution of the interfacial behaviour as a function of time, but this does not seem a very realistic proposition in the case of the engine where there are hundreds of contacts whose responses will, to some extent, interact. So, it would be valuable to be able to predict the steady state response without tracking out the

transient, if this is possible. The analogy between frictional slip and plastic slip is quite strong insofar as frictional slip is an orthogonal process *within the slip plane*, but not in an overall sense. The question as to whether Melan’s elastic–plastic shakedown theorem (*‘if a residual stress state may be found which, together with the applied stress, lies always within the yield (or frictional slip) boundary, shake down to an elastic (or fully stuck) condition will occur’*) applies to frictional contacts was probed analytically from basic principles by [1] as well as [2]. It was concluded that the Melan theorem would apply to frictional contacts only when there is ‘no coupling’, that is, where a change in interfacial slip displacements produces no change in the normal contact tractions, and vice versa. Uncoupled contacts strictly arise only when the bodies pressed together are geometrically the same and made from the same material (i.e. where the contact surface is a plane of symmetry), but this statement is almost true for any incomplete contact which is capable of idealisation within the framework of a half-plane (space), provided Dundurs’ elastic mismatch parameter  $\beta = 0$ . Other contacts can be expected to show at least some degree of coupling.

Incomplete contacts can never achieve a shaken down state because the contact pressure always falls smoothly to zero near the edge, so that it is impossible to inhibit all slip. Equally, complete contacts are either fully stuck at their edges from the outset or have a very complicated local edge behaviour involving a very small region of local separation [3] and so neither class represents a good problem to study the shakedown behaviour within the context of a strongly coupled contact capable of analytical attack. Therefore, in this paper we study the problem depicted in Fig. 1, which does have all the right characteristics.

\* Corresponding author.

E-mail address: [nils.cwiekala@eng.ox.ac.uk](mailto:nils.cwiekala@eng.ox.ac.uk) (N. Cwiekala).

<https://doi.org/10.1016/j.mechrescom.2022.103958>

Received 16 November 2021; Received in revised form 1 August 2022; Accepted 3 August 2022

Available online 6 August 2022

0093-6413/© 2022 The Author(s). Published by Elsevier Ltd. This is an open access article under the CC BY license (<http://creativecommons.org/licenses/by/4.0/>).

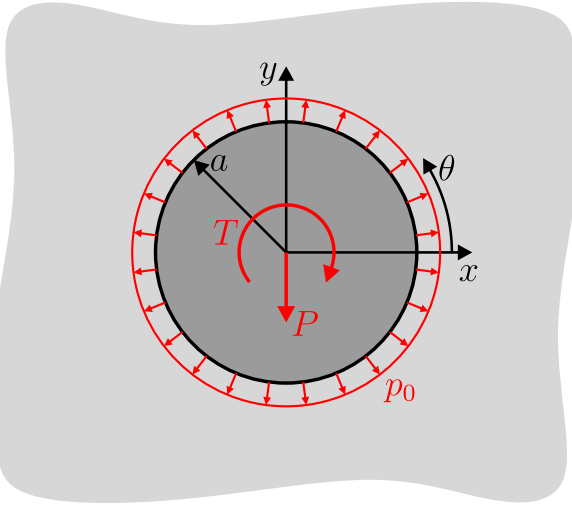


Fig. 1. Shrink fitted disk in an infinite plane with a hole.

## 2. Problem statement

With an elastic disk of radius  $a$  fitted into a circular hole in an infinite plate, the problem shows similarities to that of a circular inclusion studied by [4,5] (among others). The essence of the ‘inclusion problem’ typically is the elastic mismatch, representing a source of coupling. Here, we assume both bodies to be elastically similar, such that the geometry is the sole source of coupling. The hole is slightly smaller than the disk so that an interfacial contact pressure of magnitude  $p_0$  is developed, constant around the circumference, where both surfaces are assumed to be smooth. We start from this axisymmetric state of stress and apply a force,  $P$ , in the  $\theta = 3\pi/2$  direction as well as a torque of magnitude  $T$ , positive in the sense shown, at the origin.

### 2.1. The bilateral solution

Initially, we assume that the interface remains stuck, so that the change in the state of stress due to these loads is the same as that in a monolithic infinite body. The contact tractions,

$$p(\theta) = -\sigma_{rr}(a, \theta); \quad q(\theta) = -\sigma_{r\theta}(a, \theta)$$

can therefore be found as [6]

$$p(\theta) = p_0 - \frac{\kappa + 3}{\kappa + 1} \frac{P}{2\pi a} \sin \theta \quad (1)$$

$$q(\theta) = -\frac{T}{2\pi a^2} - \frac{\kappa - 1}{\kappa + 1} \frac{P}{2\pi a} \cos \theta, \quad (2)$$

where  $\kappa$  is Kolosov’s constant, defined as

$$\kappa = \begin{cases} 3 - 4\nu & \text{for plane strain,} \\ \frac{3-\nu}{1+\nu} & \text{for plane stress,} \end{cases}$$

and  $\nu$  is Poisson’s ratio. Slip is avoided provided that, for all  $\theta$ ,

$$|q(\theta)| < f p(\theta), \quad (3)$$

where  $f$  is the coefficient of friction. Using Eqs. (1), (2), we can express inequality (3) as

$$\left(\frac{\kappa + 3}{\kappa + 1}\right) f \tilde{P} \sin \theta \pm \left[\left(\frac{\kappa - 1}{\kappa + 1}\right) \tilde{P} \cos \theta + \tilde{T}\right] < 2\pi f, \quad (4)$$

where

$$\tilde{P} = \frac{P}{p_0 a}; \quad \tilde{T} = \frac{T}{p_0 a^2} \quad (5)$$

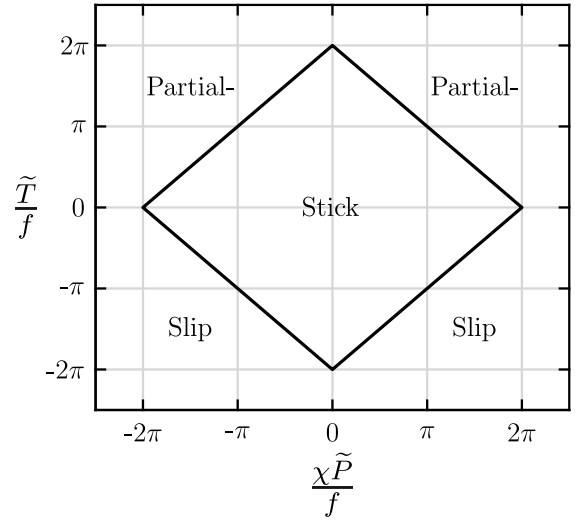


Fig. 2. Boundaries of the stick region in normalised  $P$ - $T$ -space.

are the normalised radial load and torque, respectively. The left-hand side of this inequality varies sinusoidally with  $\theta$ , and elementary calculations show that it will be satisfied for all  $\theta$  if and only if

$$\chi |\tilde{P}| + |\tilde{T}| < 2\pi f, \quad (6)$$

where the dimensionless parameter

$$\chi = \sqrt{\left(\frac{\kappa - 1}{\kappa + 1}\right)^2 + f^2 \left(\frac{\kappa + 3}{\kappa + 1}\right)^2}. \quad (7)$$

This condition allows us to identify the region of full-stick in normalised load space, as shown in Fig. 2.

If  $\tilde{P} > 0$ , and  $\tilde{T} > 0$ , the inequality (4) can be expressed as

$$\cos(\theta - \alpha) < \lambda \equiv \frac{2\pi f - \tilde{T}}{\chi \tilde{P}}, \quad (8)$$

where

$$\alpha = \arctan\left(f \frac{\kappa + 3}{\kappa - 1}\right); \quad 0 < \alpha < \frac{\pi}{2} \quad (9)$$

Corresponding results for cases where  $\tilde{P}$  and/or  $\tilde{T}$  are negative can be determined from symmetry arguments. If  $\lambda > 1$ , the inequality (8) is satisfied for all  $\theta$ , so  $\lambda = 1$  defines the boundary of the full stick region in Fig. 2. If  $\tilde{P}$  and  $\tilde{T}$  are increased so as to cross this boundary,  $\lambda$  will decrease and slip will commence at the point  $\theta = \alpha$ , which is independent of the actual values of  $\tilde{P}$  and  $\tilde{T}$ .

### 2.2. Memory-free states

If we start from the origin and cross the stick region boundary in Fig. 2 to an exterior point  $\{\tilde{P}, \tilde{T}\}$ , some slip must occur, which we characterise by the slip displacement

$$h(\theta) = u_\theta(a^+, \theta) - u_\theta(a^-, \theta). \quad (10)$$

Generally, the distribution of slip displacement, and therefore the state of stress, will depend on the exact loading path  $\mathbf{r}(t) = \{\tilde{P}(t), \tilde{T}(t)\}$  we take from the origin to the point  $\{\tilde{P}, \tilde{T}\}$ , where  $t$  denotes time. However, there exists a subset of ‘memory-free’ paths  $\mathbf{r}_C(t)$  for which the final state is not loading-history dependent. A primary purpose of the present paper is to characterise the conditions that must be met for a particular loading path to be memory free, and also to investigate the states reached when these conditions are not met.

In frictional problems, the system memory resides in the non-zero slip displacements  $h$  in stick regions that satisfy the inequality (3) in

the strict sense. Thus, if a state at  $\{\tilde{P}, \tilde{T}\}$  was reached by a memory-free load path, it must satisfy the linear complementary [LCP] condition

$$h(\theta)(|q(\theta)| - f p(\theta)) = 0, \quad (11)$$

for all  $\theta$ . In other words, the interface is partitioned into a stick region, where there is no slip displacement, and a slip region throughout which there is incipient slip with  $q(\theta) = \pm f p(\theta)$ . States that do not satisfy this condition exhibit regions that slipped during a previous segment of the load path, but which are now strictly below the incipient slip condition.

For a given point  $\{\tilde{P}, \tilde{T}\}$  there exists one and only one memory-free state  $S_C(\tilde{P}, \tilde{T})$ . In other words, the boundary-value problem has a unique solution of which the mathematical formulation is described in the next section.

### 3. Formulation for partial slip

Partial slip — i.e. slip in part but not all of the interface  $0 \leq \theta < 2\pi$  — can be described by superposing distributions of Volterra edge dislocations at the interface on the bilateral solution of Section 2.1. We define the distributions  $B_\theta(\phi), B_r(\phi)$  such that in the infinitesimal interval  $\theta = [\phi, \phi + \delta\phi]$  we have dislocations with Burgers vector components

$$\begin{aligned} b_\theta &= B_\theta(\phi) \delta\phi \quad \text{and} \\ b_r &= B_r(\phi) \delta\phi. \end{aligned} \quad (12)$$

Since the materials of the disk and the surrounding space are the same, we use the solution for a dislocation in an infinite plane (see e.g. [7]). In particular, it can be shown that a concentrated dislocation  $\{b_\theta, b_r\}$  located at  $(a, \phi)$  induces tractions  $\{q(\theta), p(\theta)\}$  at  $(a, \theta)$  given by

$$\begin{Bmatrix} q(\theta) \\ p(\theta) \end{Bmatrix} = \frac{2\mu}{\pi(\kappa+1)a} \begin{bmatrix} K_{q\theta} & K_{qr} \\ K_{p\theta} & K_{pr} \end{bmatrix} \begin{Bmatrix} b_\theta(\phi) \\ b_r(\phi) \end{Bmatrix}, \quad (13)$$

where  $\mu$  is the modulus of rigidity and

$$\begin{aligned} K_{q\theta}(\theta, \phi) &= K_{pr}(\theta, \phi) = \frac{\sin(\theta - \phi) \cos(\theta - \phi)}{2(1 - \cos(\theta - \phi))} \\ K_{qr}(\theta, \phi) &= -\frac{1}{2} \cos(\theta - \phi) \\ K_{p\theta}(\theta, \phi) &= \frac{1}{2} (\cos(\theta - \phi) + 2). \end{aligned} \quad (14)$$

Although the state of stress induced by these dislocations is independent of the path cut, the line of the cut must be chosen so that it follows the line of discontinuity of displacements, i.e. the interface between the two bodies. On the other hand, the path cut has to go to infinity at some point, so it cannot follow the interface exclusively. The problem is similar to that in a crack problem, where the path cut must follow the crack up to the tip after which it can go to infinity by any arbitrary path, because we impose a closure condition.

In this paper, we restrict attention to cases in which the radial force is insufficient to cause separation, so the radial component of displacement is continuous across the interface, the only discontinuity being that in the tangential direction. For this case, the dislocation distributions and the slip displacement are related by the equations [8]

$$B_\theta(\phi) = \frac{1}{a} \frac{dh(\phi)}{d\phi}; \quad B_r(\phi) = -\frac{h(\phi)}{a} \quad (15)$$

and hence

$$B_\theta(\phi) + \frac{dB_r}{d\phi} = 0 \quad (16)$$

The contact tractions due to fairly general dislocation distributions can be obtained by convolution on Eq. (13). After superposing the bilateral solution (1), (2), we obtain

$$\begin{aligned} p(\theta) &= p_0 - \frac{\kappa+3}{\kappa+1} \frac{P}{2\pi a} \sin(\theta) \\ &+ \frac{2\mu}{\pi(\kappa+1)} \int_{\eta_1}^{\eta_2} [B_\theta(\phi) K_{p\theta}(\theta, \phi) + B_r(\phi) K_{pr}(\theta, \phi)] d\phi \end{aligned} \quad (17)$$

$$\begin{aligned} q(\theta) &= -\frac{T}{2\pi a^2} - \frac{\kappa-1}{\kappa+1} \frac{P}{2\pi a} \cos(\theta) \\ &+ \frac{2\mu}{\pi(\kappa+1)} \int_{\eta_1}^{\eta_2} [B_\theta(\phi) K_{q\theta}(\theta, \phi) + B_r(\phi) K_{qr}(\theta, \phi)] d\phi, \end{aligned} \quad (18)$$

where we note that dislocations are present only in the slip zone, defined here as  $\eta_1 < \phi < \eta_2$ .

#### 3.1. Slip condition

In the slip zone, the contact tractions must satisfy the equality  $q(\theta) = \pm f p(\theta)$  and if slip is generated as a result of crossing the boundary in the quadrant in Fig. 2 corresponding to  $P, T > 0$ , we must take the negative sign. Eqs. (17), (18) with the notation of Eqs. (5), (7), (9) then yield the dimensionless singular integral equation

$$\int_{\eta_1}^{\eta_2} \hat{B}_\theta(\phi) [K_{q\theta} + f K_{p\theta}] + \hat{B}_r(\phi) [K_{qr} + f K_{pr}] d\phi = \frac{1}{4} (\cos(\theta - \alpha) - \lambda) \quad (19)$$

where

$$\hat{B}_i(\phi) = \frac{\mu}{(\kappa+1)} \frac{B_i(\phi)}{p_0 \chi \tilde{P}}, \quad (20)$$

$i = r, \theta$ , and we have omitted the arguments  $(\theta, \phi)$  on  $K_{p\theta}$  etc. for brevity.

Throughout this analysis, we have assumed that there is a single slip zone, but if  $T = 0$ , the problem is symmetrical about the  $y$ -axis in Fig. 1 and first slip will be determined by the development of two symmetrically disposed slip zones on either side of  $\theta = \pi/2$ .

We also need to satisfy the closure condition

$$\int_{\eta_1}^{\eta_2} \hat{B}_\theta(\phi) d\phi = 0, \quad (21)$$

which serves to determine the extent of the slip zone.

### 4. Numerical solution of the integral equation

After normalising the integral range via

$$2\phi = (\eta_2 - \eta_1)s + (\eta_2 + \eta_1) \quad \text{and} \quad (22)$$

$$2\theta = (\eta_2 - \eta_1)t + (\eta_2 + \eta_1) \quad (23)$$

(see [9]), the singular integral Eq. (19) can be solved numerically. We employ the Gauss–Chebyshev quadrature introduced by [10]. Bounded behaviour is enforced at both ends of the slip zone by extracting the factor  $\omega(s) = \sqrt{1-s^2}$  from the solution,  $B_i(s) = \omega(s)\psi_i(s)$ . The resulting system of  $N+1$  equations have to fulfil the slip condition at the  $N$  integration points  $s_j$ . The condition to preserve radial displacement continuity (16) provides another equation at each of the  $N$  integration points. In discretised form, this reads

$$\omega(s_j)\psi_r(s_j) = \frac{\pi}{2}(\eta_2 - \eta_1) \sum_{m=1}^j W_m \psi_\theta(s_m), \quad (24)$$

where the weights,  $W_m$ , are given in [8]. The presence of the unknown angles  $\eta_1$  and  $\eta_2$  makes the system of  $2N+1$  equations for the  $2N$  unknowns  $\psi_\phi(s_j)$  and  $\psi_r(s_j)$  (as well as the angles  $\eta_1$  and  $\eta_2$ ) nonlinear. We follow the procedure described in [9,11] by adding a dummy variable,  $\psi_d$ , to each of the  $N+1$  equations expressing the slip condition. The resulting system of equations is linear in the  $2N+1$  unknowns  $\psi_\phi(s_j)$ ,  $\psi_r(s_j)$  and  $\psi_d$ , and can be inverted for a given choice of  $\eta_1$  and  $\eta_2$ . Employing a minimisation algorithm, we may then find the specific combination of  $\eta_1$  and  $\eta_2$ , for which  $\psi_d = 0$  and Eq. (21) is fulfilled. Notice that, provided the function  $\psi_i(s)$  is a polynomial, for a sufficiently high number of integration points,  $N$ , the Gauss–Chebyshev quadrature will return exact values at the points  $s_j$  [8]. Here, convergence was reached for  $N = 80$  integration points.

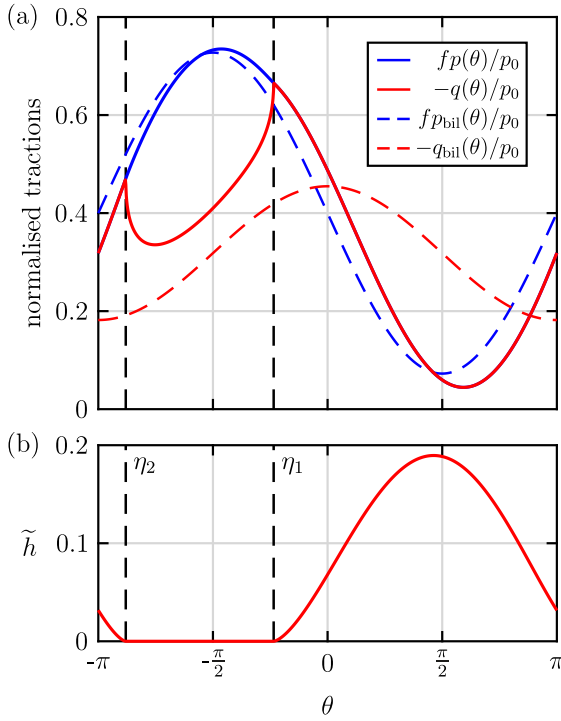


Fig. 3. (a) Normal and shear traction for  $\tilde{P} = 3$  and  $\tilde{T} = 2$  shown as solid lines, with bilateral solution as dashed lines and (b) normalised tangential slip displacement along the circumference (plane strain with  $\nu = 0.3$ ,  $f = 0.4$ ).

## 5. Partial slip results

Fig. 3(a) shows the contact tractions  $p(\theta), q(\theta)$  for the case where  $\tilde{P} = 3$  and  $\tilde{T} = 2$  in Fig. 2. The dashed lines show the bilateral tractions of Eqs. (1), (2) and the solid lines show the tractions as modified by partial slip. Notice that the normal tractions are presented through the combination  $fp(\theta)$  since this expression also defines the shear tractions in the slip zone. Fig. 3(b) shows the corresponding normalised slip displacement

$$\tilde{h}(\theta) = \frac{\mu h(\theta)}{(\kappa + 1)p_0 a}. \quad (25)$$

Notice that the normal tractions  $p(\theta)$  are modified by partial slip, which reflects the normal–tangential coupling in this geometry. One consequence of this is that the boundary in  $\{\tilde{P}, \tilde{T}\}$  space at which partial slip gives way to separation is influenced by the coefficient of friction. The shear tractions  $q(\theta)$  represent a much larger deviation from the bilateral solution and exhibit the classical square-root bounded asymptotic behaviour at the ends of the stick zone.

## 6. Boundary of the partial slip region

If the loads  $\{\tilde{P}, \tilde{T}\}$  move further away from the stick–slip boundary in Fig. 2, eventually the partial slip state must transition either to full slip, or to a state involving partial slip and separation.

For full slip, we have  $q(\theta) = \pm f p(\theta)$  for all  $\theta$  and the torque can be obtained as

$$T = a^2 \int_0^{2\pi} q(\theta) d\theta = \pm f a^2 \int_0^{2\pi} p(\theta) d\theta. \quad (26)$$

Substituting for  $p(\theta)$  from (17) and evaluating the integrals, we obtain

$$T = \pm 2\pi f p_0 a^2 \quad \text{or} \quad \tilde{T} = \pm 2\pi f, \quad (27)$$

since the other terms in (17) integrate to zero. For example

$$\int_0^{2\pi} \int_0^{2\pi} B_i(\phi) K_{ji}(\theta, \phi) d\phi d\theta = \int_0^{2\pi} B_i(\phi) \int_0^{2\pi} K_{ji}(\theta, \phi) d\theta d\phi. \quad (28)$$

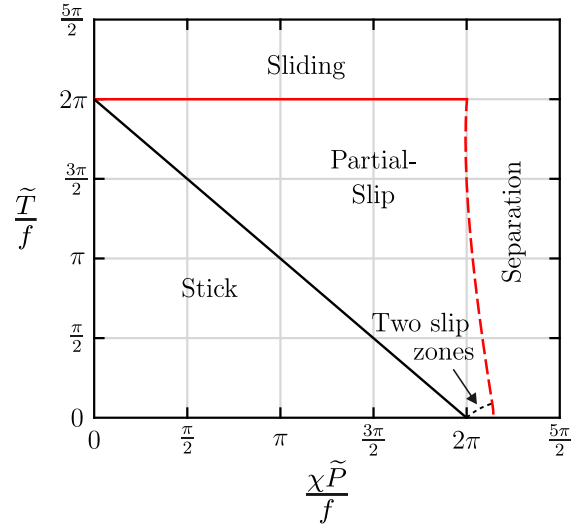


Fig. 4. Limit state boundaries in normalised  $P$ - $T$ -space taking effects of partial slip into consideration (plane strain with  $\nu = 0.3$ ,  $f = 0.4$ ).

The inner integral is zero from (14) except for the case  $j = p$ ,  $i = \theta$ , where the closure condition ensures that the outer integral is zero. Thus the full slip boundary depends only on the applied torque  $T$  and is independent of  $P$ . This boundary is defined by horizontal solid lines at  $\tilde{T}/f = \pm 2\pi$  in Fig. 2, and it corresponds to the condition  $\lambda = 0$ , where  $\lambda$  is defined in Eq. (8).

By contrast, the shape of the separation boundary depends on the coefficient of friction, the result for  $f = 0.4$  and  $\nu = 0.3$  being shown in Fig. 4. This dependence is relatively weak, but we also note that if  $\tilde{T} \ll \tilde{P}$ , memory free loading paths can be found in which a second ‘detached’ slip zone develops before separation. This range occupies a larger part of the load space at lower values of  $f$ .

## 7. The incremental problem

In this section, we pose the question “What conditions must be satisfied by a load path  $r(t)$  in order that it be memory-free – i.e.  $r \in r_c$ ?”

Suppose we have reached a given point  $\{\tilde{P}, \tilde{T}\}$  by a memory-free path and we now make an infinitesimal change in the loads to  $\{\tilde{P} + \delta\tilde{P}, \tilde{T} + \delta\tilde{T}\}$ . This new state will also be memory free if and only if the LCP condition (11) is satisfied for all  $\theta$  during the loading increment. In particular, (i) the slip boundaries  $\eta_1, \eta_2$  must not recede, and (ii) the slip displacement  $\tilde{h}(\theta)$  must not decrease at any point in the slip zone. If condition (ii) is not satisfied, a stick region will develop from the point of first violation.

We first note that the governing integral Eq. (19) depends on the loads only through the parameter  $\lambda$  defined in Eq. (8). Fig. 5 shows the evolution of the slip region as we move from the stick boundary  $\lambda = 1$  to the full slip boundary  $\lambda = 0$ . Notice that both boundaries advance as  $\lambda$  is decreased, so a necessary condition for a memory-free path is that  $d\lambda/dt \leq 0$ . Fig. 6 shows contours of constant slip extent, and hence of constant  $\lambda$ . Eq. (8) shows that these contours are all straight lines passing through the point  $(0, 2\pi)$ . Thus, if we are instantaneously at a point on one of the contours, the memory-free condition requires that subsequent motion be directed into the region above and to the right of that contour.

For a given value of  $\lambda$ , the dislocation distributions  $B_i(\phi)$  and hence the slip displacements  $\tilde{h}(\theta)$  are proportional to  $\tilde{P}$ , from Eq. (20). It follows that if we move along one of the lines of constant  $\lambda$  in Fig. 6 in the direction of decreasing  $\tilde{P}$ , the slip zone extent will remain constant, but the slip displacement will decrease for all  $\theta$ , violating the LCP condition (11). Thus a more stringent condition than  $d\lambda/dt \leq 0$  must be

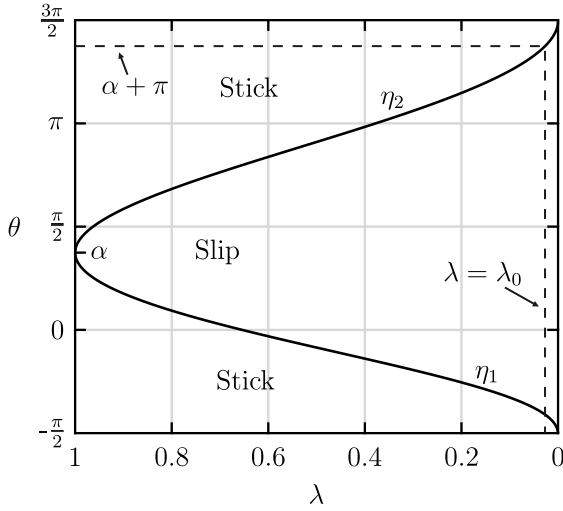


Fig. 5. Evolution of the slip zone as the loading parameter  $\lambda$  is reduced (plane strain with  $\nu = 0.3$ ,  $f = 0.4$ ).

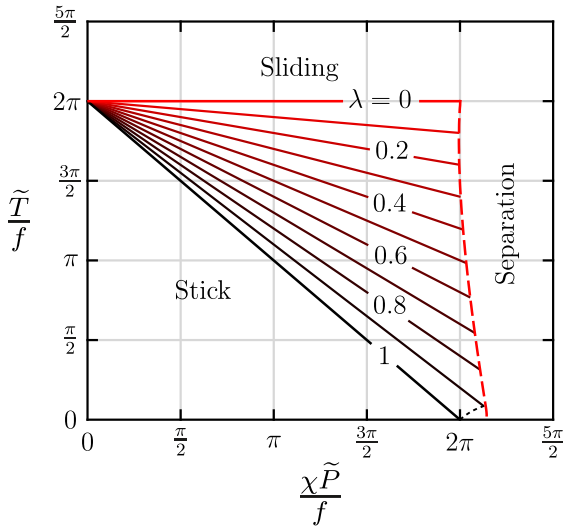


Fig. 6. Contours of  $\lambda$  and hence of constant slip extent.

imposed to ensure that the loading path is memory free in cases where  $\tilde{P}$  is decreasing. This condition can be determined by choosing the loading direction such that all points in the instantaneous slip region continue to slip, except for one point at which the slip velocity is zero. Fig. 7 shows a set of contours such that to satisfy this condition when  $\tilde{P} < 0$ , these contours must be crossed from below in order that the state remain memory-free. This stationary point is found to be very close to the point of maximum slip displacement which itself moves only very slightly in the range  $(\alpha, \pi/2)$  over the entire partial-slip load range.

## 8. Transition to full stick

If we reach a memory-free state in the partial slip region and then move beyond it, the possible incremental states are characterised by the four regions identified in Fig. 8. Incremental changes heading into region II will result in a continued memory-free state, the right and left boundaries of this region being defined by the slope of the corresponding contour in Figs. 6 and 7 respectively.

There also exists a range of loading directions, labelled I in Fig. 8, for which the contact will transition to complete stick, and indeed this state would then persist for a finite load increment in the same

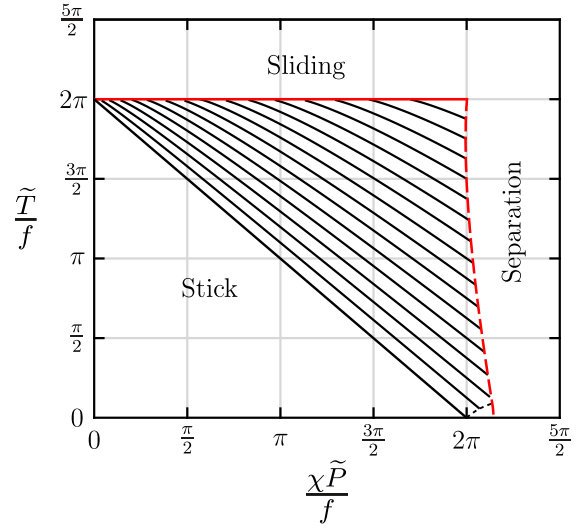


Fig. 7. Contours which must be crossed from below to ensure a memory-free state when  $\tilde{P} < 0$  (plane strain with  $\nu = 0.3$ ,  $f = 0.4$ ).

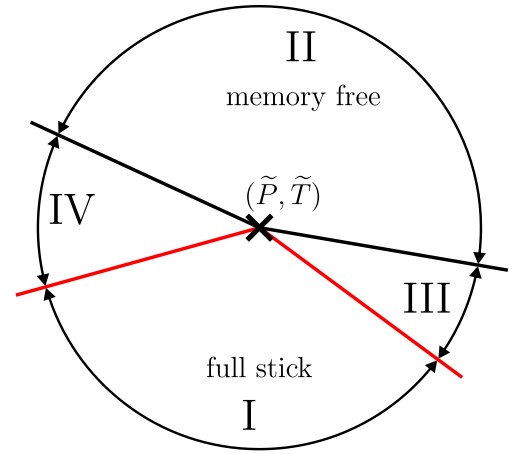


Fig. 8. Incremental loading pointing into region II in normalised  $P$ - $T$ -space will preserve a memory-free state. Region I corresponds to a transition to full stick.

direction. If incremental full stick occurs, the changes in traction will be given by the bilateral solution. If  $\tilde{P}$  continues to increase, the boundary between regions I and III in Fig. 8 must therefore have the same slope as the original stick-slip boundary in Figs. 4, 6 and 7, since below this line, the increment in  $q(\theta)$  is in the same direction as the instantaneous value and is lower than the increment in  $f p(\theta)$  for all  $\theta$  and vice versa.

If  $\tilde{P}$  decreases, the maximum value of  $[f \delta p(\theta) - \delta q(\theta)]$  occurs at  $\theta = \alpha + \pi$ . This point will lie inside the original partial slip zone if  $\eta_2 > \alpha + \pi$ , and hence if  $\lambda < \lambda_0$ , where  $\lambda_0$  is defined by the construction in Fig. 5 and also corresponds to points above the black dashed line in Fig. 9 for plane strain with  $\nu = 0.3$ ,  $f = 0.4$ . In this range, the boundary between I and IV in Fig. 8 is symmetrical to that between I and III — i.e. it has the same slope but opposite sign.

For  $\lambda > \lambda_0$  and  $\tilde{P}$  decreasing, the point most liable to slip will be adjacent to  $\theta = \eta_2$ , where  $\eta_2$  is defined in Fig. 5. It can be shown that additional partial slip will occur if

$$\frac{1}{\chi} \frac{d\tilde{T}}{d\tilde{P}} > -\cos(\eta_2 - \alpha). \quad (29)$$

Fig. 9 shows a set of contours such that the slope of the I/III boundary at any given point is that of the contour through that point. The limiting condition  $\lambda = \lambda_0$  is plotted as a black dashed line.



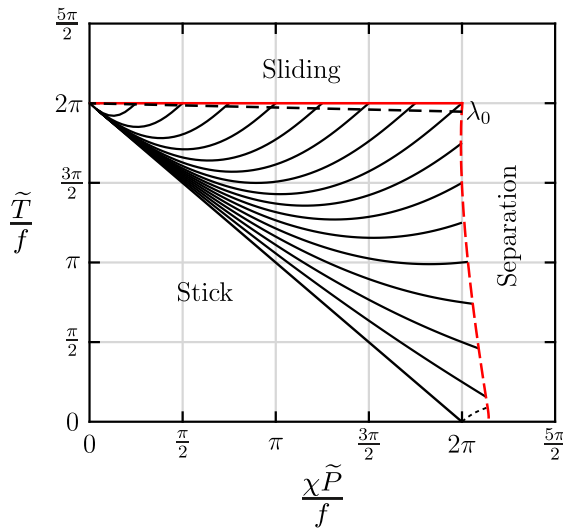


Fig. 9. Contours defining the slope of the I/IV boundary in Fig. 8 (plane strain with  $\nu = 0.3$ ,  $f = 0.4$ ).

## 9. Conclusions

We have studied the problem of a disc, shrink-fitted into an infinite plane with a circular hole and subjected to a radial force and a torque. This problem differs from most of the analytical contact mechanics literature in that there is strong coupling between frictional slip displacements and normal tractions – a factor which is known to influence history-dependence in frictional contact problems. In this paper we have defined the conditions under which the state reached is ‘memory-free’, i.e. independent of the precise loading path. We find that this condition is satisfied provided that the slope of the path in  $\{\tilde{P}, \tilde{T}\}$  space always lies in the region II of Fig. 8, whose boundaries are defined by the slopes of the contours in Figs. 6 and 7. We also define the conditions under which a loading increment will result in the entire interface transitioning to stick. The results provide a starting point for a future study of the shakedown behaviour of a continuous coupled contact.

## Declaration of competing interest

The authors declare the following financial interests/personal relationships which may be considered as potential competing interests: Nils Cwiekala reports financial support was provided by Rolls Royce plc. David Hills reports financial support was provided by Rolls Royce plc.

## Data availability

No data was used for the research described in the article.

## Acknowledgements

N. Cwiekala and D. A. Hills thank Rolls-Royce plc and the EPSRC for the support under the Prosperity Partnership Grant ‘Cornerstone: Mechanical Engineering Science to Enable Aero Propulsion Futures’, Grant Ref: EP/R004951/1.

## References

- [1] A. Klarbring, M. Ciavarella, J. Barber, Shakedown in elastic contact problems with Coulomb friction, *Int. J. Solids Struct.* 44 (25–26) (2007) 8355–8365.
- [2] J.R. Barber, A. Klarbring, M. Ciavarella, Shakedown in frictional contact problems for the continuum, *C. R. Méc.* 336 (1–2) (2008) 34–41.
- [3] C. Churchman, D. Hills, General results for complete contacts subject to oscillatory shear, *J. Mech. Phys. Solids* 54 (6) (2006) 1186–1205.
- [4] L.M. Keer, J. Dundurs, K. Kiattikomol, Separation of a smooth circular inclusion from a matrix, *Internat. J. Engrg. Sci.* 11 (11) (1973) 1221–1233.
- [5] P. Kelly, D.A. Hills, D. Nowell, Curved interface cracks between elastically dissimilar media, with application to the analysis of circular inclusions, *Int. J. Mech. Sci.* 36 (3) (1994) 173–181.
- [6] J.R. Barber, *Elasticity*, Vol. 172, 2010.
- [7] J. Weertman, *Dislocation Based Fracture Mechanics*, World Scientific Publishing Company, 1996.
- [8] D.A. Hills, P. Kelly, D. Dai, A. Korsunsky, *Solution of Crack Problems: The Distributed Dislocation Technique*, Vol. 44, Springer Science & Business Media, 1996.
- [9] M. Comninou, The interface crack in a Shear field, *J. Appl. Mech.* 45 (2) (1978) 287–290.
- [10] F. Erdogan, G.D. Gupta, On the numerical solution of singular integral equations, *Quart. Appl. Math.* 29 (4) (1972) 525–534.
- [11] M. Comninou, The interface crack, *J. Appl. Mech.* 44 (4) (1977) 631–636.